NUCL SCI TECH (2017) 28:103
DOI 10.1007/s41365-017-0248-1

Implementation of a cusp-like for real-time digital pulse shaper in nuclear spectrometry

Jun Liu[1] · Jian Yang[1] · Guo-Qiang Zeng[1] · Kai-Qi Zhang[1] · Shi-Long Wei[1] · Liang-Quan Ge[1]

Received: 18 July 2016 / Revised: 11 September 2016 / Accepted: 15 September 2016 / Published online: 8 June 2017

Abstract Pulse shaping, which improves signal-to-noise ratio excellently, has been extensively used in nuclear signal processing. This paper presents a cusp-like pulse-shaping technique developed through the recursive difference equation in time domain. It can be implemented in field programmable gate array hardware system. Another flat-topped cusp-like shaper is developed to optimize the time constant of pulse shaping and reduce the influence of ballistic deficit. The methods of both baseline restoration and pile-up rejection are described. The ^{137}Cs energy spectra measured with the digital cusp-like shaper are 6.6% energy resolution, while those by traditional analog pulse shaper are 7.2% energy resolution, under the same conditions. This technique offers flexibility, too, in adjusting the pulse shaper parameters.

Keywords Cusp-like · Pulse shaping · Digital signal processing · FPGA · Spectrometry

1 Introduction

Exponential pulses are essential output of nuclear detectors, which needs pulse shaping to reduce the influences of electronic noises, pulse pile-up and ballistic deficit on energy resolution [1–3]. Traditional methods of pulse shaping include quasi-Gaussian shaper, triangular shaper, trapezoidal shaper and so on [4–6]. From the theory of optimal pulse shaping, the ideal infinite cusp-like shape gives the best signal-to-noise ratio (SNR), but it is not practical for a hardware system to form such a pulse shape, because theoretically this needs an infinite time duration [1, 7]. However, the cusp-like shape of finite time duration, which is good enough to achieve much better filtering effect than trapezoidal pulse shaping, can be implemented in the real-time hardware with low-scale logic units only [5, 8]. In this paper, we study the synthesis of the finite cusp-like and flat-topped cusp-like shaper for high-energy-resolution applications. This algorithm can effectively substitute the complex analog pulse-shaping circuits and improve the system performances on both pulse throughput and energy resolution.

2 Pulse shaper systems

Traditional analog pulse shaping is carried out through the analog circuits, as shown in Fig. 1a. The peak detect and hold circuits are used to capture the maximum amplitudes of the pulse signals [9, 10]. Then, these amplitudes are converted into corresponding channels of energy spectrum by the low-speed ADC. Figure 1b shows the method of digital pulse shaping. The original nuclear pulses are digitized by the high-speed ADC. The outputs of pulse shaping are obtained in real-time by FPGA's powerful parallel processing capacity [11, 12]. Digital pulse shaping is better than analog pulse shaping in reducing influences of both electronic noises and temperature [13].

This work was supported by the National Natural Science Foundation of China (Nos. 41474159 and 41504139), Sichuan Youth Science and Technology Foundation (No. 2015JQ0035), Sichuan Science and Technology Support Program (No. 2017GZ0390) and the Key Laboratory of Applied Nuclear Techniques in Geosciences Sichuan (No. gnzds2014006).

✉ Guo-Qiang Zeng
24829500@qq.com

[1] Chengdu University of Technology, Chengdu 610059, China

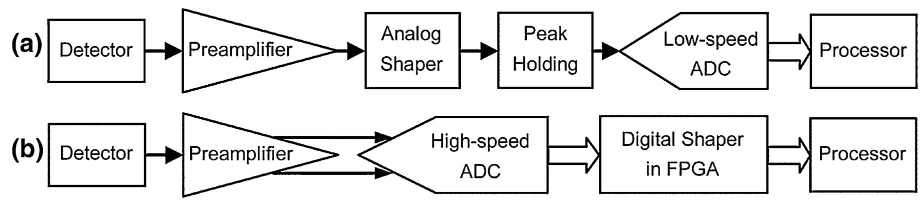

Fig. 1 Analog (**a**) and digital (**b**) pulse-shaping systems

Hence, digital pulse processing method is used for cusp-like shaper in this study. In addition, digital integrator reduces the demands of both ADC's differential nonlinearity and integral nonlinearity.

3 Cusp-like algorithm

3.1 Traditional algorithm

Outputted by a typical radiation detector, a nuclear pulse is a bi-exponential signal with a sharp rising edge and a relatively slow falling-edge. It is fitted frequently by functions of the uni-exponential model and the bi-exponential model [14]. In this paper, the pulse signal is characterized by a uni-exponential,

$$s(t) = A \times \exp(-t/\tau), \tag{1}$$

where A is the pulse amplitude and τ is the time constant of the pulse falling-edge. As shown in Fig. 2, the traditional pulse shaping obtains the cusp-like shape through the convolution of the original pulse and the impulse response function of the cusp-like shaper. In fact, this shaper works as a digital finite impulse response (FIR) filter [6, 11, 15].

The discrete equation of convolution is:

$$y[n] = s[n] * h[n] = \sum_{k=0}^{N-1} a_k s[n-k], \tag{2}$$

where a_k are the coefficients of the filter, $N = \tau_s/T_s$ is the number of coefficients with τ_s being the finite time of $y[n]$, and T_s is the sampling period. This convolution needs too many multiplication and memory units to be practical.

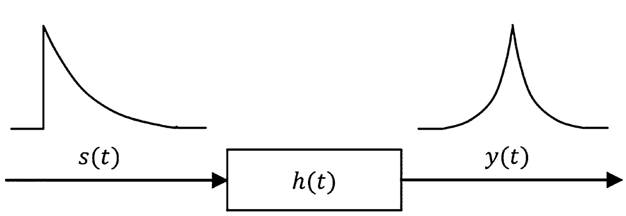

Fig. 2 Transfer function model of cusp-like pulse shaping

3.2 Recursive algorithm

We use the algorithm of cusp-like pulse shaping based on the recursive difference equations in time domain. This recursive algorithm is suitable for real-time implementation in hardware system [16]. As shown in Fig. 3, the decayed tails of original pulse signal $s[n]$ are removed to obtain the impulse signal $\delta[n]$ through deconvolution. Then, $\delta[n]$ is synthesized to the pulse sequence $p[n]$ through the operations of both delay and reverse. A symmetrical T-shaped pulse $q[n]$ is obtained by the integration of $p[n]$. The continuous integration of $q[n]$ can obtain a bipolar triangular pulse $r[n]$. Lastly, the cusp-like shape $y[n]$ can be obtained by the integration of $r[n]$.

Current pulses of a nuclear detector are not ideal as they have a certain lasting time. The partial electric charges are dissipated in the charge collection. Ballistic deficit and charge trapping effects can noticeably reduce energy resolution of spectrometers when shapers producing short pulses with sharp peaks are used. It has been demonstrated that the effects can be reduced by using flat-topped shapes [3, 5]. Therefore, it is necessary to design a cusp-like shaper with the finite flat-top. As long as the width of flat-top is greater than the lasting time of the current pulse, the flat-topped cusp-like shaper can effectively overcome the ballistic deficit. Equations (3–7) are recursive difference equations of cusp-like and flat-topped cusp-like pulse shaping.

$$\delta[n] = s[n] - d \times s[n-1], \tag{3}$$

$$\begin{aligned} p[n] =& (\delta[n] - \delta[n-A] + \delta[n-A-B-1] \\ & - \delta[n-2A-B-1]) \\ & - A \times (\delta[n-A] - \delta[n-A-1] + \delta[n-A-B] \\ & - \delta[n-A-B-1]), \end{aligned} \tag{4}$$

$$q[n] = q[n-1] + p[n], \tag{5}$$

$$r[n] = r[n-1] + q[n], \tag{6}$$

$$y[n] = y[n-1] + r[n], \tag{7}$$

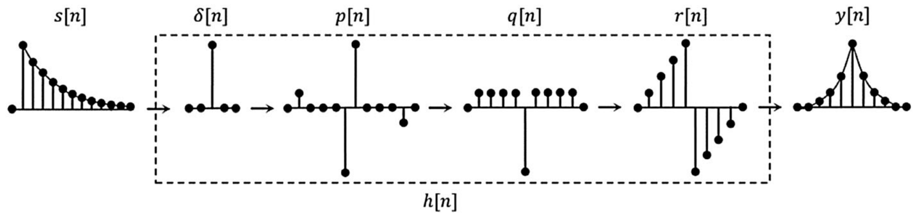

Fig. 3 Recursive method of cusp-like pulse shaping using difference equations

where $d = \exp(-T_s/\tau)$, with T_s being the ADC sampling period, A is the number of points on the rising edge, and B is the number of points on the flat-top. When B is not equal to 0, it is a flat-topped cusp-like shaper.

4 Simulation

Simulink is the simulation environment of MATLAB, which can be applied for algorithm development and numerical calculation [17]. The data of original signals form FPGA are loaded into MATLAB's workspace, and then, a *from workspace* module is used to import the data into Simulink. The logic diagram in the Simulink is drawn according to the recursive difference equations, as shown in Fig. 4. In the difference equations, the exponential pulse is converted into a unit impulse. This processing must use an accurate shaping time constant τ to guarantee no undershoot and trails in pulse shaping. The flat-top of cusp-like shaper plays a crucial role in selecting an optimal shaping time constant τ by judging whether the flat-top is parallel to the baseline [6, 16].

Figure 5 shows an ideal exponential pulse of 2-μs decayed time constant and the corresponding flat-topped cusp-like pulse shaping with varied shaping time constants τ. A large τ causes the baseline undershoot, and the corresponding flat-top will tilt toward the lower right, while a small τ makes the baseline lifting, and the corresponding flat-top will tilt toward the upper right. In those cases, both

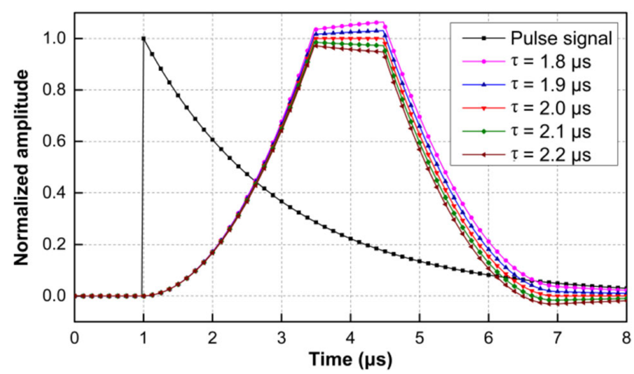

Fig. 5 (Color online) Results of flat-topped cusp-like shaper ($A = 100$, $B = 40$) with varied time constants

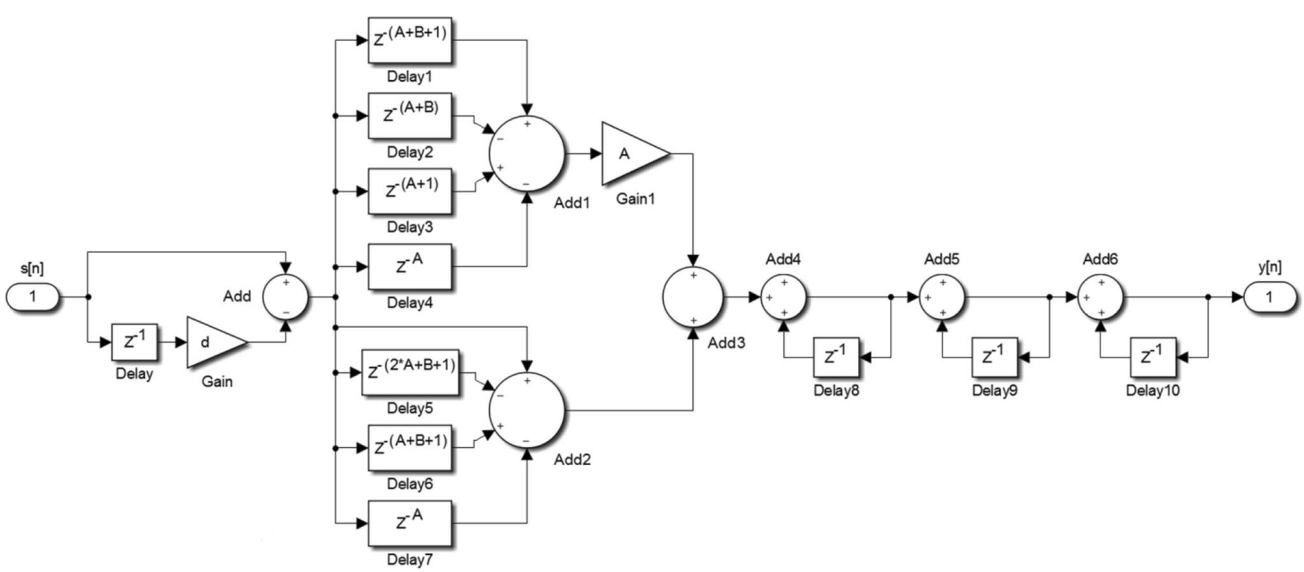

Fig. 4 The logic diagram of cusp-like shaper in Simulink

baseline and peak extraction will would be affected. Therefore, by judging the obliquity of between flat-top and baseline, the optimal shaping time constant can be effectively chosen to obtain the optimal cusp-like shape.

5 Experiments and performances

5.1 Implementation in hardware system

The low power dissipation AD9224 (12-Bit and 40 MSPS, Analog Devices, Inc.) and low-cost EP4CE6 series FPGA (Altera) are used in this paper, which are the good trade-off between the cost and performances. For convenience in high-speed ADC sampling, the original pulse signals from nuclear detectors are adjusted by the signal conditioning circuits. Then, the FPGA is used to implement the digital pulse processing algorithm by its parallel operation. The modules of pulse height analyzer (PHA) in FPGA consist of data buffers, cusp-like shaper, pile-up rejection, baseline restorer, amplitude extraction, external interface and so on [12, 18]. In addition, a parameter module, which is a register array, stores the parameters of other modules. The parameters of pulse shaping can be modified by changing the registers. The logic diagram of cusp-like pulse-shaping algorithm in FPGA is shown in Fig. 6.

The parameter d in Eq. (3) is a constant float-point type, but the float-point operations in FPGA should be avoided, for saving the operation speed and data memory volume. This parameter can be converted into a fraction, so that the float-point operations can turn into integer multiplication and integer division.

In the experiment, a NaI(Tl) crystal (ϕ 76 mm $\times$ 76 mm) coupled with a PMT (76 mm CR160-01, Hamamatsu) is used as the front-end detector, and a ^{137}Cs source is placed at 10 cm away from the detector.

5.2 Ballistic deficit correction

To verify whether the cusp-like shaper in FPGA hardware is consistent with the theoretical design, SignalTap logic analyzer is used to analyze the real-time data in FPGA memory through a JTAG hardware debugger. Figure 7 shows an original pulse signal, the corresponding cusp-like pulse shaping ($A = 120$, $B = 0$) and the flat-topped cusp-like pulse shaping ($A = 100$, $B = 40$). Due to influence of the lasting time of current pulse, the rising edge of original pulse is not fast enough, hence the ballistic deficit in the corresponding cusp-like pulse shaping. For the flat-topped cusp-like shaper, its height gradually increases accompanying the collection of electric charges, and would reach the maximum value at completion of the charges collection. Hence, the flat-topped cusp-like shaper can eliminate the influence of amplitude deficit. The average of flat-top can be set as the peak value, which can further reduce the influence of noise. However, the over-large flat-top width would increase the probability of pulse pile-up, so the trade-off of between ballistic deficit and pulse pile-up should be carefully considered.

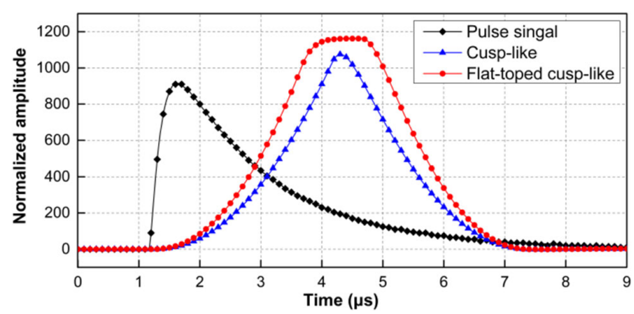

Fig. 7 (Color online) Original pulse and cusp-like pulse shaping form FPGA

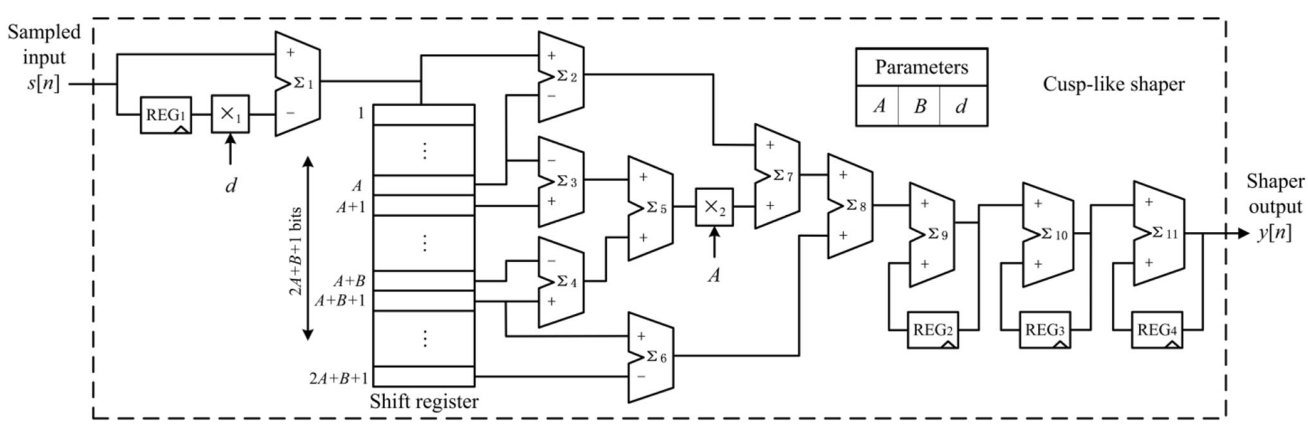

Fig. 6 The logic diagram of cusp-like pulse-shaping algorithm in FPGA

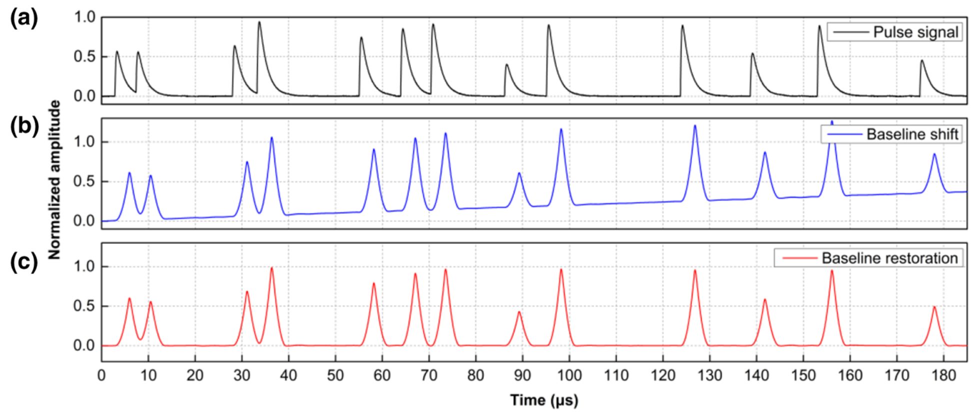

Fig. 8 (Color online) The original pulse signals (**a**), baseline drift of pulse shaping (**b**) and baseline restoration after adjusting the order of transfer functions (**c**)

5.3 Baseline drift restoration

Figure 8a, b shows the original pulse signals and the cusp-like pulse shaping, but its baseline gradually drifts over the time. Since the recursive process of pulse shaping performs the differential operations firstly, it would amplify the noises from the original pulse signals. Particularly the colored noises, whose spectral density is not flat, would gradually accumulated so as to the baseline shift [18]. Thus, all the differential operations must be placed at the final stage by changing the order of transfer functions in the linear system. Figure 8c shows the improved baseline fluctuates in a small range of a long-term test. Besides, the large numeric value can be obtained through the integration operations, which effectively reduce the round-off error of division operations in the back-stage.

5.4 Pile-up rejection

Under high count rates, pulse pile-up is serious. The pile-up rejection method plays an important role in distinguishing the dead-time signals whose peak intervals are less than half of the shaping time constant. The fast pulse shaping can generate an ultra-narrow pulse signal by using a very small shaping time constant, which can be used for pile-up rejection. As the ultra-narrow pulse signal position

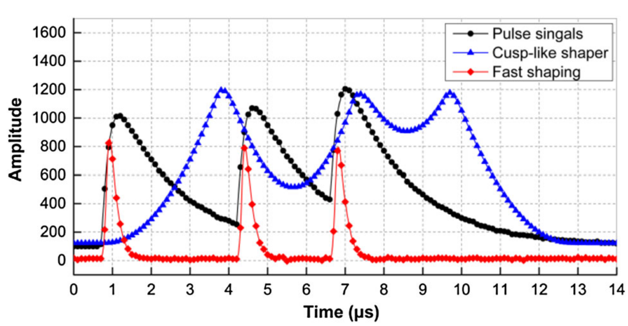

Fig. 9 (Color online) The pile-up correction method of the cusp-like shaper

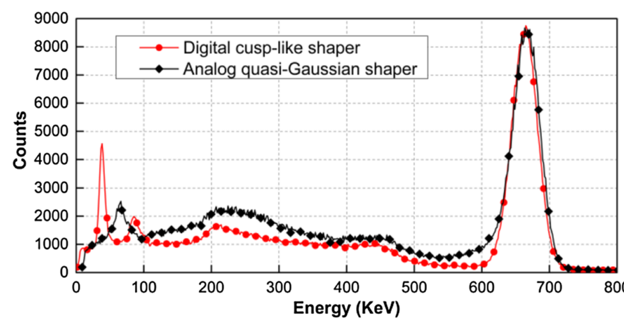

Fig. 10 (Color online) Measured energy spectrum of ^{137}Cs by using analog quasi-Gaussian shaper and digital cusp-like shaper

is the same as the rise edge of its corresponding original pulse signal, a threshold can be set to trigger this ultra-narrow pulse signal. Figure 9 shows the pulse pile-up of three signals, the cusp-like pulse shaping ($A = 120$, $B = 0$, $\tau = 6$ μs) and the ultra-narrow pulse signals of the fast pulse shaping ($A = 6$, $B = 0$). It can be seen that the time intervals of the firstly two ultra-narrow pulses are greater than 3 μs, so the first cusp-like shape can be used for peak extraction. However, the last two ultra-narrow pulses are gapped by less than 3 μs, so the two pulse signals should be discarded during amplitude extraction and only can be used for pulse count.

5.5 Energy spectrum measurement

Energy spectra of the ^{137}Cs source measured by traditional analog quasi-Gaussian shaper and the digital cusp-like shaper are shown in Fig. 10. The FWHM of photoelectric peak at 662 keV is 7.2 and 6.6% for the analog quasi-Gaussian shaper and the digital cusp-like shaper, respectively. The analog pulse shaper has no immunity to ballistic deficit so that its energy spectrum of photoelectric peak at 662 keV has serious asymmetry tails. Besides, as it is susceptible to noises, a higher pulse triggering threshold is set to reduce the error counts in low-energy region, and thus, the X-ray peak of ^{137}Ba, which is the decay product of

^{137}Cs, cannot be detected. However, the digital flat-topped cusp-like shaper overcomes the ballistic deficit, presents the clear Compton scattering spectrum, detects the X-ray peak of ^{137}Ba and has good linearity.

6 Conclusion

In this work, we studied a digital cusp-like pulse-shaping algorithm which used recursive difference equations. In actual hardware system, the flat-topped cusp-like shaper can be used to effectively select the optimal shaping time constant and eliminate the influences of the ballistic deficit. Besides, the baseline drift can be restored by adjusting the order of transfer functions, and the fast pulse-shaping method can be used for pile-up rejection. Finally, this algorithm is implemented in FPGA. Compared with traditional analog shaper, digital cusp-like shaper has great improvement in energy resolution. Hence, it can effectively substitute the traditional analog pulse shaper and be used for high-precision nuclear spectrometry systems.

References

1. V. Radeka, Optimum signal-processing for pulse-amplitude spectrometry in the presence of high-rate effects and noise. IEEE Trans. Nucl. Sci. **15**, 455–470 (1968). doi:10.1109/TNS.1968.4324970
2. C. Imperiale, A. Imperiale, On nuclear spectrometry pulses digital shaping and processing. Measurement **30**, 49–73 (2001). doi:10.1016/S0263-2241(00)00057-9
3. L. Fabris, J.A. Becker, F.S. Goulding et al., Simultaneous ballistic deficit immunity and resilience to parallel noise sources: a new pulse shaping technique. IEEE Trans. Nucl. Sci. **48**, 450–454 (2001). doi:10.1109/23.940098
4. V.T. Jordanov, Real time digital pulse shaper with variable weighting function. Nucl. Instrum. Methods Phys. Res. A **505**, 347–351 (2003). doi:10.1016/S0168-9002(03)01094-5
5. V.T. Jordanov, G.F. Knoll, Digital synthesis of pulse shapes in real time for high resolution radiation spectroscopy. Nucl. Instrum. Methods Phys. Res. A **345**, 337–345 (1994). doi:10.1016/0168-9002(94)91011-1
6. A. Regadio, S. Sanchez-Prieto, M. Prieto et al., Implementation of a real-time adaptive digital shaping for nuclear spectroscopy. Nucl. Instrum. Methods Phys. Res. A **735**, 297–303 (2014). doi:10.1016/j.nima.2013.09.063
7. P.W. Nicholson, *Nuclear electronics* (Wiley, New York, 1974)
8. M. Bogovac, C. Csato, Implementation of a truncated cusp filter for real-time digital pulse processing in nuclear spectrometry. Nucl. Instrum. Methods Phys. Res. A **694**, 101–106 (2012). doi:10.1016/j.nima.2012.07.042
9. G.D. Geronimo, P. O'Connor, A. Kandasamy, Analog CMOS peak detect and hold circuits. Part 1. Analysis of the classical configuration. Nucl. Instrum. Methods Phys. Res. A **484**, 533–543 (2002). doi:10.1016/S0168-9002(01)02059-9
10. P. Seller, A.L. Hardie, Q. Morrissey, Noise distribution of a peak track and hold circuit. Nucl. Instrum. Methods Phys. Res. A **696**, 129–135 (2012). doi:10.1016/j.nima.2012.08.048
11. P.S. Lee, C.S. Lee, J.H. Lee, Development of FPGA-based digital signal processing system for radiation spectroscopy. Radiat. Meas. **48**, 12–17 (2013). doi:10.1016/j.radmeas.2012.11.018
12. J.B. Simoes, C.M.B.A. Correia, Pulse processing architectures. Nucl. Instrum. Methods Phys. Res. A **422**, 405–410 (1999). doi:10.1016/S0168-9002(98)00992-9
13. R. Grzywacz, Applications of digital pulse processing in nuclear spectroscopy. Nucl. Instrum. Methods Phys. Res. B **204**, 649–659 (2003). doi:10.1016/S0168-583X(02)02146-8
14. G.F. Knoll, *Radiation detection and measurement*, 3rd edn. (Wiley, New York, 1999)
15. V.T. Jordanov, Exponential signal synthesis in digital pulse processing. Nucl. Instrum. Methods Phys. Res. A **670**, 18–24 (2012). doi:10.1016/j.nima.2011.12.042
16. J. Lanchares, O. Garnica, J.L. Risco-Martin et al., Real-time evolvable pulse shaper for radiation measurements. Nucl. Instrum. Methods Phys. Res. A **727**, 73–83 (2013). doi:10.1016/j.nima.2013.05.164
17. W.Y. Xiao, Y.X. Wei, X.Y. Ai et al., System simulation of digital pulse spectrometer. Nucl. Instrum. Methods Phys. Res. A **555**, 231–235 (2005). doi:10.1016/j.nima.2005.09.027
18. S. Buzzetti, M. Capou, C. Guazzoni et al., High-speed FPGA-based pulse-height analyzer for high resolution X-ray spectroscopy. IEEE Trans. Nucl. Sci. **52**, 854–860 (2005). doi:10.1109/TNS.2005.852699